Article

Immunity

Endoplasmic Reticulum Stress Activates the Inflammasome via NLRP3- and Caspase-2-Driven Mitochondrial Damage

Graphical Abstract

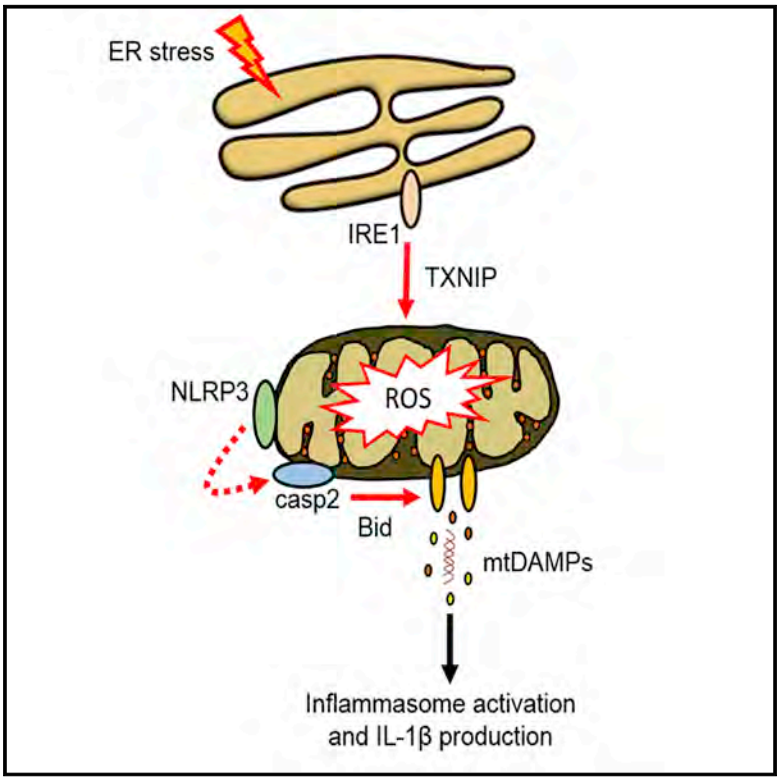

Authors

Denise N. Bronner, Basel H. Abuaita, Xiaoyun Chen, ..., Yongqun He, Xiao-Ming Yin, Mary X.D. O'Riordan

Correspondence

oriordan@umich.edu

In Brief

The endoplasmic reticulum stress response modulates inflammatory responses during chemical stress or microbial infection. O'Riordan and colleagues report that endoplasmic reticulum stress sensor IRE1α induces ROS-dependent NLRP3 translocation to mitochondria. NLRP3 stimulates the caspase-2-Bid mitochondrial damage pathway, leading to release of mitochondrial danger signals that activate the inflammasome.

Highlights

- Infection-associated ER stress initiates mitochondrial damage through IRE1α
- Mitochondrial damage is required for IRE1α-dependent IL-1β production
- IRE1α promotes mitochondrial damage via NLRP3, caspase-2, and Bid
- The NLRP3-caspase-2 axis drives general ER stress-induced inflammasome activation

Bronner et al., 2015, Immunity *43*, 451–462
September 15, 2015 ©2015 Elsevier Inc.
http://dx.doi.org/10.1016/j.immuni.2015.08.008

Immunity
Article

Endoplasmic Reticulum Stress Activates the Inflammasome via NLRP3- and Caspase-2-Driven Mitochondrial Damage

Denise N. Bronner,[1] Basel H. Abuaita,[1] Xiaoyun Chen,[2] Katherine A. Fitzgerald,[3] Gabriel Nuñez,[4,5] Yongqun He,[1,5,6] Xiao-Ming Yin,[2] and Mary X.D. O'Riordan[1,5,*]
[1]Department of Microbiology and Immunology, University of Michigan Medical School, Ann Arbor, MI 48109, USA
[2]Department of Pathology and Laboratory Medicine, Indiana University School of Medicine, Indianapolis, IN 46202, USA
[3]Division of Infectious Diseases and Immunology, Department of Medicine, University of Massachusetts Medical School, Worcester, MA 01605, USA
[4]Department of Pathology, University of Michigan Medical School, Ann Arbor, MI 48109, USA
[5]Comprehensive Cancer Center, University of Michigan Medical School, Ann Arbor, MI 48109 USA
[6]Unit for Laboratory Animal Medicine, University of Michigan Medical School, Ann Arbor, MI 48109 USA
*Correspondence: oriordan@umich.edu
http://dx.doi.org/10.1016/j.immuni.2015.08.008

SUMMARY

Endoplasmic reticulum (ER) stress is observed in many human diseases, often associated with inflammation. ER stress can trigger inflammation through nucleotide-binding domain and leucine-rich repeat containing (NLRP3) inflammasome, which might stimulate inflammasome formation by association with damaged mitochondria. How ER stress triggers mitochondrial dysfunction and inflammasome activation is ill defined. Here we have used an infection model to show that the IRE1α ER stress sensor regulates regulated mitochondrial dysfunction through an NLRP3-mediated feed-forward loop, independently of ASC. IRE1α activation increased mitochondrial reactive oxygen species, promoting NLRP3 association with mitochondria. NLRP3 was required for ER stress-induced cleavage of caspase-2 and the pro-apoptotic factor, Bid, leading to subsequent release of mitochondrial contents. Caspase-2 and Bid were necessary for activation of the canonical inflammasome by infection-associated or general ER stress. These data identify an NLRP3-caspase-2-dependent mechanism that relays ER stress to the mitochondria to promote inflammation, integrating cellular stress and innate immunity.

INTRODUCTION

Cellular stress provokes release of molecular danger signals that stimulate inflammatory signaling (Kono and Rock, 2008; Zhang et al., 2013), but the mechanisms linking stress with release of danger-associated molecular patterns (DAMPs) are not fully defined. Such mechanisms are relevant to human health as molecular stress and inflammation increase with age and are associated with many acute and chronic diseases (Brown and Naidoo, 2012; Davis et al., 2011; Hao et al., 2013; Tan et al., 2013). Mitochondria can act as platforms to nucleate signaling by large molecular complexes, like the nucleotide-binding domain and leucine-rich repeat containing (NLRP3) inflammasome, and drive inflammation through release of mitochondrial DAMPs in response to diverse stressors (Subramanian et al., 2013). How such distinct stressors as infection, glucose deprivation, oxidative stress, or disruption of calcium homeostasis trigger these inflammatory events is unclear. The endoplasmic reticulum (ER) is a large endomembrane compartment that is highly sensitive to perturbation and is central to the function of many organelle networks, suggesting that ER might act as a relay station between stressors and mitochondria, linking stress and inflammatory signaling.

Three ER-resident unfolded protein sensors, IRE1α (IRE1), ATF6, and PERK control the ER stress response, an adaptive program that defines the fate of the stressed cell (Hetz, 2012). Toll-like receptors (TLR), which primarily recognize microbial ligands like lipopolysaccharide (LPS), selectively stimulate IRE1 (Martinon et al., 2010), and LPS-primed macrophages react to ER stressors by activating the NLRP3 inflammasome (Menu et al., 2012). Microbial infection is a useful model for investigating ER stress and inflammation because infection is often associated with ER stress, and animals deficient in components of the IRE1 signaling pathway are more susceptible to bacterial infection than controls (Bischof et al., 2008; Martinon et al., 2010; Pillich et al., 2012; Seimon et al., 2010). NLRP3-deficient animals exhibit increased susceptibility and decreased survival during infection by some microbial pathogens (von Moltke et al., 2013). *Brucella abortus* strain RB51 is an attenuated bacterial vaccine strain that infects macrophages, causes ER stress, and provokes a robust immune response without the complex effects of intracellular replication (Li and He, 2012). We therefore used RB51 as a probe to elucidate ER stress-dependent immune signaling. Virulent *B. abortus* mediates inflammasome activation through NLRP3 (Gomes et al., 2013), suggesting that *B. abortus* strains could be appropriate for studying the interplay between ER stress and NLRP3-dependent immune signaling (Davis et al., 2011). Notably, NLRP3 in resting cells is associated with ER, but upon stimulation moves to ER-mitochondrial junctions (Zhou et al., 2011). These data led us to hypothesize that upon

infection, ER stress sensors could modulate NLRP3-dependent crosstalk between ER and mitochondria by an as yet unidentified mechanism, leading to inflammasome activation.

RESULTS

RB51-Induced Inflammasome Activation Requires IRE1 and TXNIP

TLR ligands (e.g., LPS) activate IRE1, but not ATF6 or PERK, activating transcription of proinflammatory cytokines (Martinon et al., 2010). To determine whether IRE1 was stimulated during RB51 infection, we investigated splicing of *Xbp1* transcript, a direct target of the endonuclease domain of activated IRE1 (Hetz, 2012; Sidrauski and Walter, 1997). Tunicamycin (TM), an inhibitor of protein glycosylation (Hetz, 2012; Olden et al., 1978; Zeng and Elbein, 1995), served as a positive control for ER stress assays. Robust splicing of *Xbp1* was seen in TM-treated bone-marrow-derived macrophages (BMDM) and RB51-infected BMDM at 8 hr post-infection (pi) (Figure 1A). ER stress signaling can lead to cell death in some contexts (Lerner et al., 2012; Oslowski et al., 2012), so we measured cell death by release of lactate dehydrogenase, and found that the majority of infected cells were viable by 8 hr pi (Figure S1A). Thus, infection by RB51 stimulated IRE1 activation, as previously observed for other microbial ligands (Martinon et al., 2010).

Recent studies revealed that ER stress can drive inflammasome activation (Lerner et al., 2012). RB51 stimulated robust interleukin-1β (IL-1β) production at both low and high multiplicity of infection (MOI), and at high MOI was comparable to the positive control LPS+ATP treatment (Figure S1B). We therefore tested whether ER stress was required for RB51-induced IL-1β production. Inhibition of IRE1 with 4μ8C (Cross et al., 2012) in RB51-infected BMDM led to decreased *Xbp1* splicing and caspase-1 cleavage (Figure S1C and Figure 1B). Treatment with tauroursodeoxycholic acid (TUDCA), a molecular chaperone that alleviates ER stress, or 4μ8C, resulted in less IL-1β production in RB51-infected BMDM, but not BMDM treated with LPS+ATP, our positive control for inflammasome activation (Figure 1C). Neither TUDCA nor 4μ8C decreased bacterial uptake (Figure S1D). IRE1 inhibition did not affect *Il1b* transcription, suggesting that IRE1 signaling was not required for priming (Figure 1D). IRE1 inhibition also had no effect on LPS+ATP-induced caspase-1 cleavage and IL-1β production. These data suggest that unlike RB51, LPS+ATP does not rely on ER stress to induce IL-1β production. Like IRE1 inhibition, silencing of *Ern1*, the gene that encodes IRE1 (Figure S1E and F), decreased *Xbp1* splicing, caspase-1 cleavage and IL-1β production in RB51-infected BMDM. To determine whether IRE1 modulates inflammation in vivo, we treated C57BL/6 mice with either vehicle control or 4μ8C, and infected animals intraperitoneally with 10^8 CFU of RB51. Consistent with our in vitro findings, 4μ8C-treated mice showed significantly less serum IL-1β and increased bacterial burden (Figure 1E and Figure S1G). These data point to IRE1 as an important regulator of ER stress-induced inflammasome activation during infection.

Previous studies identified multiple targets for the IRE1 endonuclease, including *Xbp1* and miR-17, a negative regulator of thioredoxin-interacting protein (TXNIP) translation (Lerner et al., 2012; Yoshida et al., 2001). The XBP1 transcription factor selectively enhances transcription of pro-inflammatory cytokine genes (Martinon et al., 2010). IRE1-dependent miR-17 degradation increases TXNIP protein, which shuttles to mitochondria and binds thioredoxin-2, raising concentrations of mitochondrial reactive oxygen species (ROS) (Lerner et al., 2012). To assess whether XBP1 or TXNIP controls IRE1-driven IL-1β production, we transfected BMDM with *Xbp1* or *Txnip* specific siRNA, infected with RB51 and measured supernatant IL-1β. Transient silencing of *Xbp1* had no effect on RB51-induced IL-1β production (Figure 1F), while silencing of *Txnip* led to reductions in IL-1β and ROS in infected BMDM (Figures 1G and 1H). These data indicate that during infection-induced ER stress, IRE1 acts through TXNIP to induce IL-1β production.

ER Stress-Induced Mitochondrial Dysfunction Aids in Inflammasome Activation

ER stress drives mitochondria to release mitochondrial-derived damage associated molecular patterns (mtDAMPs), which can activate the inflammasome (Iyer et al., 2013; Nakahira et al., 2011; Zhou et al., 2011). Previous studies have shown that TXNIP shuttling to mitochondria increases mtROS (Saxena et al., 2010). We observed increased ROS over time in RB51-infected BMDM, a phenotype dependent upon both IRE1 and TXNIP (Figure 1H). To determine whether mtROS was required for IRE1-induced IL-1β production, we infected BMDM derived from transgenic mice that express a mitochondrial-targeted catalase (mCAT) (Lee et al., 2010). Both ROS and IL-1β decreased in infected mCAT BMDM compared to infected WT BMDM (Figures 2A and 2B). The decreased ROS in mCAT BMDM had no effect on LPS+ATP-induced IL-1β production, consistent with previous work showing that mitochondrial function is not essential for activation of the NLRP3 inflammasome (Muñoz-Planillo et al., 2013). Since we observed increased ROS upon RB51 infection, possibly indicating mitochondrial dysfunction, we infected BMDM with RB51 and measured cytochrome c and mtDNA release. TM-treated and RB51-infected macrophages released mtDNA and cytochrome c into the cytosol, a process blocked by IRE1 inhibition or silencing (Figure 2C and Figures S2A and S2B). Since the presence of transfected mtDNA in the cytosol can stimulate IL-1β production (Nakahira et al., 2011; Shimada et al., 2012), we investigated whether release of mitochondrial components during RB51 infection contributed to IL-1β production by treating BMDM with cyclosporin A (CsA), which prevents opening of the mitochondrial permeability transition pore (Handschumacher et al., 1984). We infected BMDM with RB51 with or without CsA, and measured IL-1β production by ELISA. CsA treatment significantly decreased IL-1β in RB51-infected macrophages, even though bacterial uptake was unaffected (Figures 2D and S2C). In contrast, CsA treatment did not affect IL-1β production in LPS+ATP treated BMDM, indicating that our specific LPS+ATP treatment protocol induces IL-1β production independently of mitochondrial damage (Figure 2D). However, a different LPS+ATP treatment protocol led to markedly higher amounts of mtDNA released into the cytosol (Figure S2D), suggesting that involvement of the mitochondria in inflammasome activation by the classical activator, LPS+ATP, might depend on the extent or duration of cellular stress. Taken together, these data show that RB51-induced ER stress

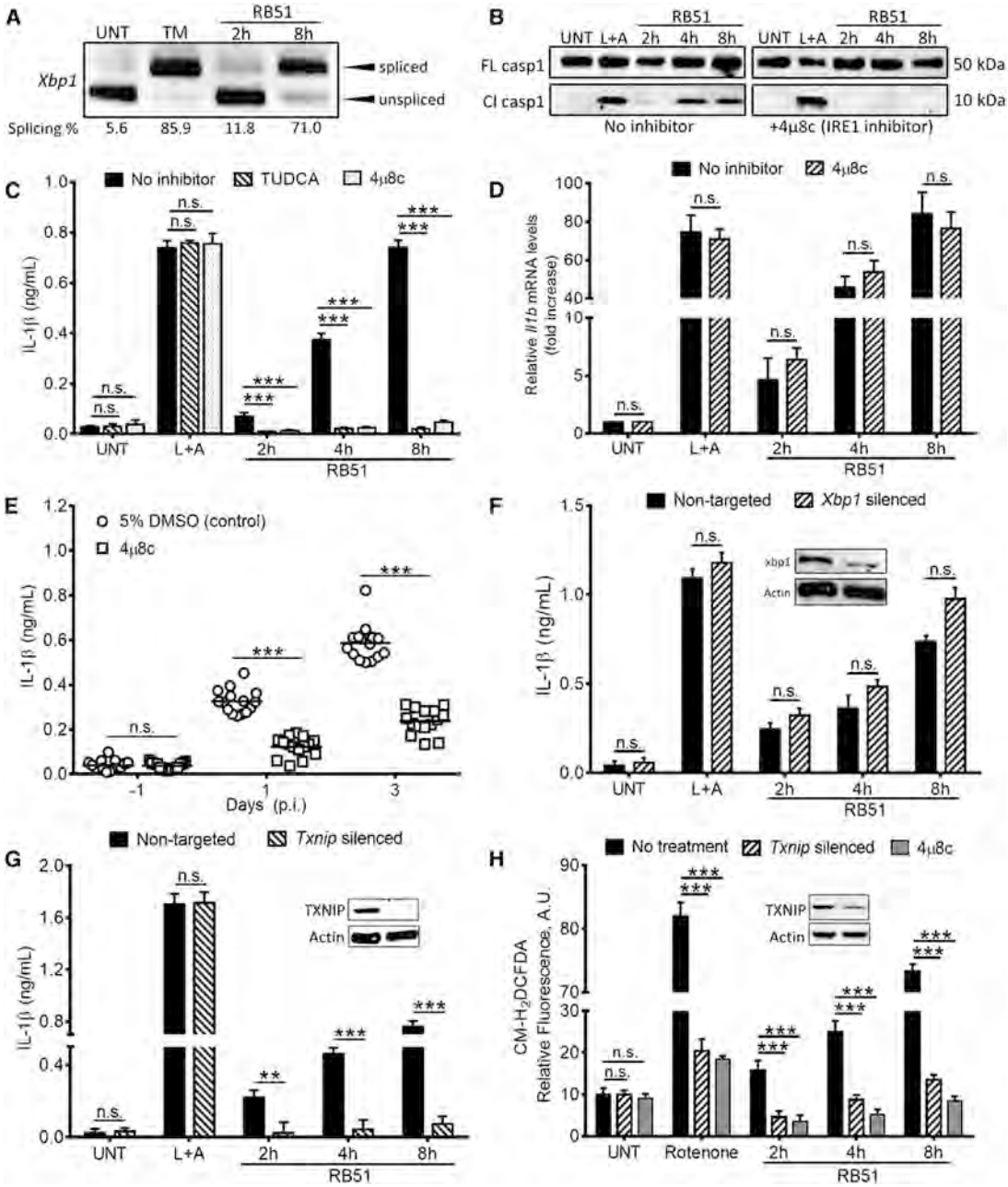

Figure 1. IRE1 Modulates Infection-Induced Inflammasome Activation via TXNIP

(A) *Xbp1* splicing, a marker of IRE1 activation, in RB51-infected BMDM. qRT-PCR samples were treated with PstI to distinguish between spliced (184 bp) and unspliced variants (119 bp following PstI digestion).

(B) Caspase-1 cleavage in RB51-infected BMDM in absence or presence of 4μ8c. Immunoblots are representative of n ≥ 3 independent experiments performed and imaged in parallel with identical parameters using a Li-Cor Odyssey imaging system.

(C) IL-1β ELISA analysis of supernatants from RB51-infected BMDM treated with or without TUDCA (chemical chaperone, 300 μM) and 4μ8c (IRE1 inhibitor, 50 μM). Error bars represent mean ± SD of n ≥ 3 independent experiments. *** represent p value < 0.0001, n.s. = not significant.

(D) qRT-PCR analysis of IL-1β transcript in RB51-infected BMDM in the absence or presence of 4μ8c.

(E) Serum IL-1β in mice treated with 5% DMSO (control, n = 15) or 4μ8c (n = 15) and infected with RB51 (i.p., CFU 1 × 10^8). Data in (E) were pooled from two independent experiments.

(F) IL-1β ELISA analysis of supernatants from RB51-infected BMDM transfected with non-targeted and *Xbp1* siRNA.

(G) IL-1β ELISA analysis of supernatants from RB51-infected BMDM transfected with non-targeted and *Txnip* siRNA.

(H) CM-H_2DCFDA was used to measure ROS during RB51 infection in presence of 4μ8c or *Txnip* siRNA. Rotenone serves as a positive control for ROS induction. Inset in (F)–(H) demonstrates silencing efficiency by immunoblot. UNT, TM, and L+A represent untreated, tunicamycin (10 μg/mL, positive control for ER stress activation) and LPS+ATP (200 ng/mL and 1mM respectively; positive control for inflammasome activation). See also Figure S1.

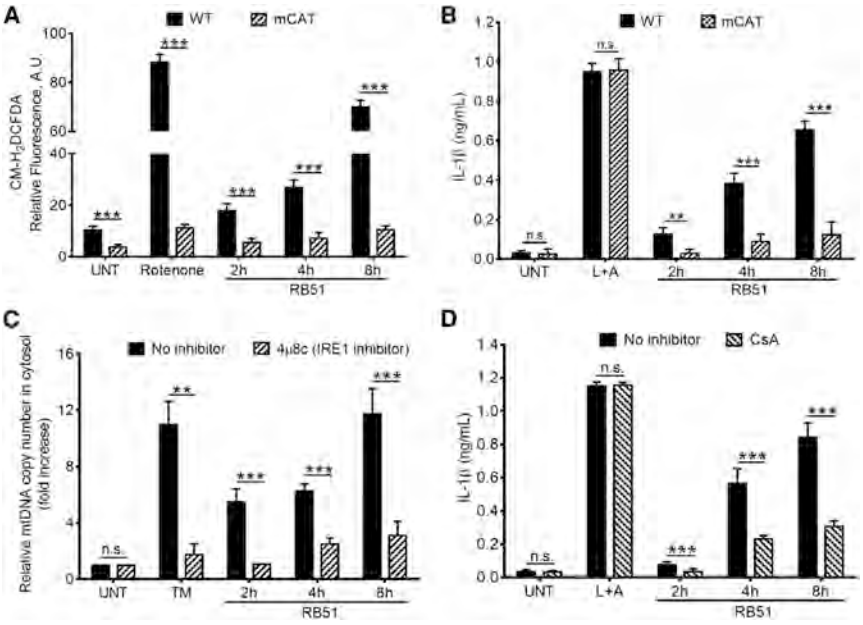

Figure 2. ER Stress-Induced Mitochondrial Dysfunction Drives IL-1β Production

(A) The ROS indicator dye, CM-H_2DCFDA, was used to measure ROS in WT and mCAT BMDM infected with RB51. Rotenone serves as a positive control for ROS induction.

(B) IL-1β concentrations in supernatants from RB51-infected WT and mCAT BMDM.

(C) qPCR analysis of mtDNA release into cytosol during RB51 BMDM infection.

(D) IL-1β concentrations in RB51-infected BMDM treated with or without cyclosporin A (CsA, 10 μM). Error bars in (A)–(D) represent mean ± SD of $n \geq 3$ independent experiments. *** represent p value < 0.0001, n.s. = not significant. UNT, TM, and L+A represent untreated and tunicamycin (10 μg/mL, positive control for ER stress activation), and 200 ng/mL LPS + 1 mM ATP (positive control for inflammasome activation). See also Figure S2.

damages mitochondria, which leads to activation of the inflammasome through an IRE1-dependent mechanism.

NLRP3 Mediates IRE1-Induced Mitochondrial Stress Independently of the ASC Inflammasome Adaptor

In macrophages infected with virulent *B. abortus*, both NLRP3 and the cytosolic DNA sensor, AIM2, were required for IL-1β production (Gomes et al., 2013). Moreover, the AIM2 inflammasome can regulate IL-1β production when stimulated by transfected mtDNA (Nakahira et al., 2011). We first assessed whether AIM2 was required for RB51-induced IL-1β production by measuring IL-1β from RB51-infected WT and *Aim2*$^{-/-}$ BMDM (Figure S3A). AIM2 did not contribute to IL-1β production induced by RB51-mediated ER stress. We then reasoned that NLRP3 would be a likely sensor to respond to the infection-induced ER stress signal. We first tested whether IRE1 signaling was required for *Nlrp3* transcription, and found that 4μ8C treatment did not alter infection-induced priming of *Nlrp3* transcription (Figure S3B). Upon activation, NLRP3 can translocate from the ER to the mitochondria (Zhou et al., 2011) and is reported to trigger mitochondrial dysfunction and IL-1β production in the presence of oxidized mtDNA (Nakahira et al., 2011; Shimada et al., 2012). To determine whether NLRP3 was involved in controlling the release of mitochondrial contents during RB51 infection, we determined whether NLRP3 was recruited to mitochondria. In RB51-infected WT BMDM, NLRP3 was recruited to the mitochondrial fraction at 4 hr pi, which corresponds with the timing of cytochrome c and mtDNA release (Figures 3A and 3B and Figure S3C). NLRP3 recruitment to the mitochondria was abolished in mCAT transgenic and *Txnip*-silenced BMDM. *Nlrp3*$^{-/-}$ macrophages did not release mtDNA nor cytochrome c into the cytosol upon RB51 infection (Figure 3C and Figure S3D). In addition, NLRP3 deficiency abolished RB51-induced IL-1β production (Figure 3D) and caspase-1 cleavage (Figure S3E), but did not affect overall caspase-1 protein amounts. Since NLRP3 appeared to be a key component of RB51-induced inflammasome activation, we investigated whether ASC or caspase-1, components of the canonical inflammasome, were also crucial to inducing mitochondrial damage. *Asc*$^{-/-}$ and YVAD-CHO (caspase-1 inhibitor)-treated BMDM were not required for mtDNA and cytochrome c release into the cytosol upon infection (Figure 3C and Figure S3F). However, ASC and caspase-1 were still necessary for IL-1β production during RB51 infection (Figure 3D). The inability to produce IL-1β in YVAD-CHO-treated macrophages was not due to decreased bacterial uptake (Figure S3G). Together, these results show that during RB51-induced inflammasome activation, NLRP3 plays a critical role in mediating release of mitochondrial contents, independently of ASC and caspase-1.

NLRP3 Drives Mitochondrial Dysfunction through Caspase-2

Under ER stress conditions, NLRP3 might facilitate release of mitochondrial contents through the cysteine protease, caspase-2. During genotoxic stress, caspase-2 can cause mitochondrial dysfunction leading to cytochrome c release (Robertson et al., 2002). Moreover, caspase-2 is activated by ER stress or RB51 infection (Chen and He, 2009; Upton et al., 2008; Upton et al., 2012), and regulates caspase-1 activation (Bronner et al., 2013; Jesenberger et al., 2000). We reasoned that under conditions of ER stress, NLRP3 might be inducing activation of caspase-2 leading to release of mtDNA and cytochrome c into the cytosol. We probed lysates from control, 4μ8C-treated, and *Ern1*-silenced (IRE1 depleted) infected macrophages, for full-length or cleaved active caspase-2 (Figure 4A and Figure S4A). IRE1 was required for caspase-2 cleavage during RB51 infection, but not for caspase-2 cleavage triggered by the genotoxic agent, etoposide (ET). To determine whether NLRP3 acted upstream or downstream of caspase-2, C57BL/6, and *Nlrp3*$^{-/-}$ BMDM were infected with RB51, and lysates probed for cleaved caspase-2 (Figure 4B). Caspase-2 cleavage was nearly absent in infected *Nlrp3*$^{-/-}$ macrophages, whereas caspase-2 cleavage in *Asc*$^{-/-}$ or caspase-1 inhibitor-treated BMDM was comparable to WT (Figure S4B). We next assessed caspase-2 mitochondrial

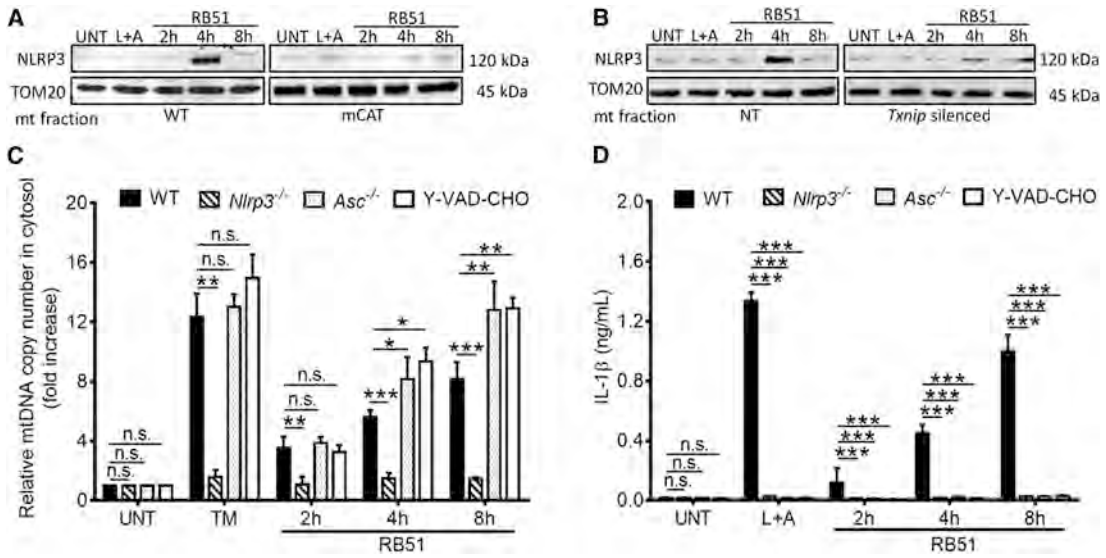

Figure 3. NLRP3 Is Required for an ER Stress-Induced Feed-Forward Loop of Mitochondria Damage

Immunoblot of NLRP3 at the mitochondrial fraction of (A) WT and mCAT BMDM and (B) non-targeted (NT) and *Txnip*-silenced BMDM.

(C) Quantitative PCR of mtDNA in cytosolic extracts from RB51-infected WT and *Nlrp3*$^{-/-}$, *Asc*$^{-/-}$, and z-YVAD-CHO (caspase-1 inhibitor, 2 μM) treated BMDM.

(D) IL-1β concentrations in RB51-infected WT and *Nlrp3*$^{-/-}$, *Asc*$^{-/-}$, and z-YVAD-CHO (caspase-1 inhibitor, 2 μM) inhibited BMDM. Error bars represent mean ± SD of n ≥ 3 independent experiments. *, **, and *** represent p values of < 0.05, < 0.001, and < 0.0001 respectively. n.s. = not significant. UNT, TM, and LPS+ATP represent untreated, tunicamycin (positive control for ER stress induction, 10 μg/mL), and LPS+ATP (positive control for inflammasome activation, 200 ng/mL, and 1 mM) respectively. Immunoblots in (A) and (B) are representative of n ≥ 3 independent experiments that were performed and imaged in parallel with identical parameters using a Li-Cor Odyssey imaging system. See also Figure S3.

recruitment and its role in mitochondrial damage. During RB51 infection, caspase-2 was recruited to mitochondria, in an IRE1- and NLRP3-dependent matter (Figures 4C and 4D). Infected *Casp2*$^{-/-}$ BMDM released less mtDNA and cytochrome c into the cytosol (Figures 4E and S4C). Moreover, caspase-2 deficiency abolished IL-1β production and caspase-1 activation without affecting bacterial uptake (Figure 4F and Figures S4D and E). Although *Casp2*$^{-/-}$ deficient BMDM were comparably infected to WT, it is possible that they were deficient in transcription of *Nlrp3* or *Il1b*. We performed quantitative RT-PCR analysis to measure *Nlrp3* and *Il1b* transcript in WT and *Casp2*$^{-/-}$ BMDM. Infected *Casp2*$^{-/-}$ BMDM produced similar amounts of *Nlrp3* and *Il1b* transcript as WT BMDM (Figure 4G and Figure S4F), suggesting that the defect in IL-1β production is not in priming but in activating the inflammasome. Similar to our in vitro data, *Casp2*$^{-/-}$ mice infected with RB51 exhibited low concentrations of serum IL-1β and higher bacterial burden (Figure 4H). These data suggest that during infection, NLRP3 can mediate ER stress-induced mitochondrial damage and inflammasome activation by a caspase-2-dependent mechanism.

NLRP3 and Caspase-2 Induce Mitochondrial Damage via the Pore-Activating Factor Bid

We aimed to elucidate the mechanism by which NLRP3 and caspase-2 could regulate mitochondrial dysfunction. NLRP3 and caspase-2 could lead to truncation and activation of Bid, which damages mitochondria by licensing pore formation of Bax, a pro-apoptotic factor of the Bcl-2 family (Korsmeyer et al., 2000). To determine whether Bid was involved in ER stress-induced mitochondrial damage, we infected 4μ8C-treated or *Ern1*-silenced (IRE1-depleted) macrophages with RB51, and probed for the presence of tBid, using etoposide as a positive control. Total Bid amounts remained constant under all conditions, but Bid truncation was diminished in 4μ8C-treated and *Ern1*-silenced macrophages (Figure 5A and Figure S5A), possibly implicating Bid in ER stress-induced mitochondrial dysfunction. ET induces mitochondrial dysfunction but does not induce ER stress (Hitomi et al., 2004; Wang et al., 1998). Therefore, it was not surprising to see that IRE1 inhibition had no effect on Bid truncation in ET-treated BMDM. To elucidate the role of NLRP3 and caspase-2 in this process, we infected C57BL/6, *Nlrp3*$^{-/-}$, and *Casp2*$^{-/-}$ BMDM with RB51, and the status of Bid was assessed by immunoblot. Bid truncation markedly decreased in the absence of NLRP3 and caspase-2 (Figure 5B and Figure S5B). Infected *Bid*$^{-/-}$ BMDM released less mtDNA into the cytosol than WT controls, confirming that Bid is required for mitochondrial damage, even though Bid-deficiency did not affect bacterial uptake (Figures 5C and S5C). *Bid*$^{-/-}$ BMDM infected with RB51 also exhibited diminished secretion of IL-1β and caspase-1 cleavage (Figures 5D and 5E). Consistent with our in vitro results, RB51-infected *Bid*$^{-/-}$ mice showed a decrease in serum IL-1β, as well as an increase in bacterial burden in the spleen, compared to wild-type controls (Figure 5F and Figure S5D). Thus, during RB51 infection, NLRP3 and caspase-2 trigger mitochondrial damage through Bid, leading to inflammasome activation.

NLRP3 and Caspase-2 Are Required for Inflammasome Activation in Response to Chemical ER Stress

Our data thus far identified the IRE1-NLRP3-caspase-2-Bid axis as a mechanism for relaying infection-induced ER stress signals to the mitochondria, leading to inflammasome activation. We

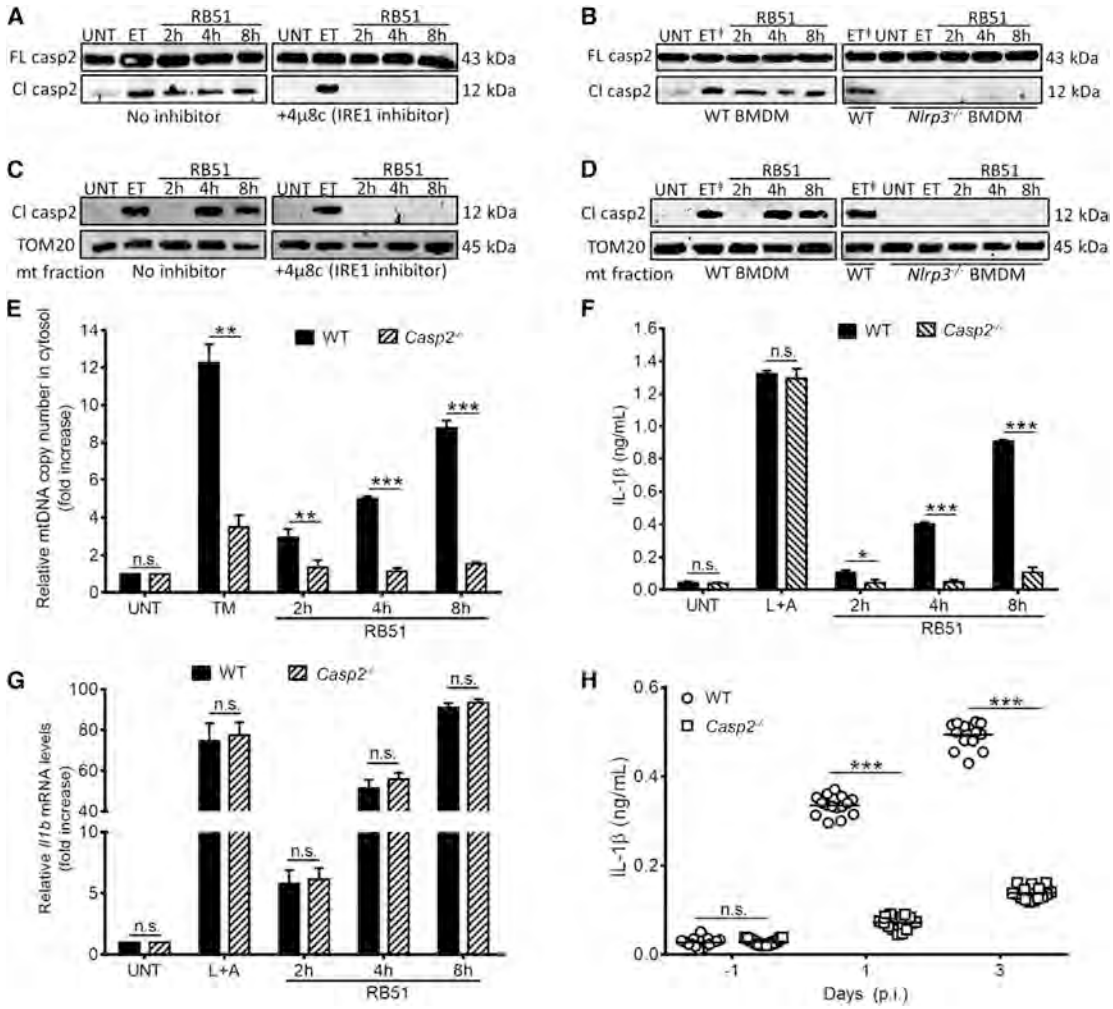

Figure 4. NLRP3 and Caspase-2 Are Required for ER Stress-Induced Inflammasome Activation

Immunoblot analysis of caspase-2 in (A) with or without 4μ8c (IRE1 inhibitor, 50 μM) and (B) RB51-infected WT and *Nlrp3*$^{-/-}$ BMDM. Immunoblot analysis of caspase-2 in the mitochondrial fraction (C) with or without 4μ8c (IRE1 inhibitor, 50 μM) and (D) RB51-infected WT and *Nlrp3*$^{-/-}$ BMDM – ET‡ identifies duplicate lanes of the same sample.

(E and F) qRT-PCR analysis of mtDNA in cytosolic fractions of infected WT and *Casp2*$^{-/-}$ BMDM (E). IL-1β concentrations in (F) WT and *Casp2*$^{-/-}$ RB51-infected (i.p., CFU 1 × 10^{8}) BMDM.

(G) qRT-PCR analysis of *Il1b* transcript in WT and *Casp2*$^{-/-}$ RB51-infected BMDM.

(H) Serum IL-1β serum by ELISA in WT (n = 15) and *Casp2*$^{-/-}$ mice (n = 15). Data in (H) were pooled from two independent experiments. Error bars represent mean ± SD of n ≥ 3 independent experiments. *, **, and *** represent p values of < 0.05, < 0.001, and < 0.0001 respectively. n.s. = not significant. UNT, ET, TM, and L+A represent untreated, etoposide (positive control for caspase-2 activation and Bid truncation, 25 μM), tunicamycin (positive control for ER stress induction, 10 μg/mL), and LPS+ATP (positive control for inflammasome activation, 200 ng/mL and 1mM respectively). Immunoblots in (A)–(D) are representative of n ≥ 3 independent experiments that were performed and imaged in parallel with identical parameters using a Li-Cor Odyssey imaging system. Full-length caspase-2 and TOM20 (mitochondrial specific outer membrane protein) serve as loading controls. See also Figure S4.

considered the possibility that this pathway might be important for infection-induced inflammasome activation, but not in the general ER stress response. We therefore tested whether IRE1, NLRP3, caspase-2, and Bid were required for inflammasome activation in response to thapsigargin (TG), tunicamycin (TM), and brefeldin A (BFA), three chemical inducers that cause ER stress by distinct mechanisms. Treatment of WT BMDM with TG, TM, or BFA resulted in robust caspase-1 cleavage but low IL-1β production, suggesting that minimal priming was occurring during TG, TM, and BFA treatment in contrast to LPS+ATP (Figures 6A and 6B). Since both priming to stimulate *Il1b* transcription and inflammasome activation are required for IL-1β secretion (Schroder and Tschopp, 2010), we assessed proIL-1β production by immunoblot and found that TM and BFA induced weak proIL-1β production whereas TG did not trigger any detectable proIL-1β production (Figure S6A). Thus, ER stress is a weak inducer of the first signal (priming) that regulates transcription of *Il1b*, but can act as a second signal for inflammasome activation. Consistent with our infection model, inhibition of IRE1 abrogated TM- or TG-induced caspase-1 cleavage (Figure 6B). Although BFA did trigger IRE1 activation as measured by X*bp1* splicing (Figure S6B), IRE1 was not required

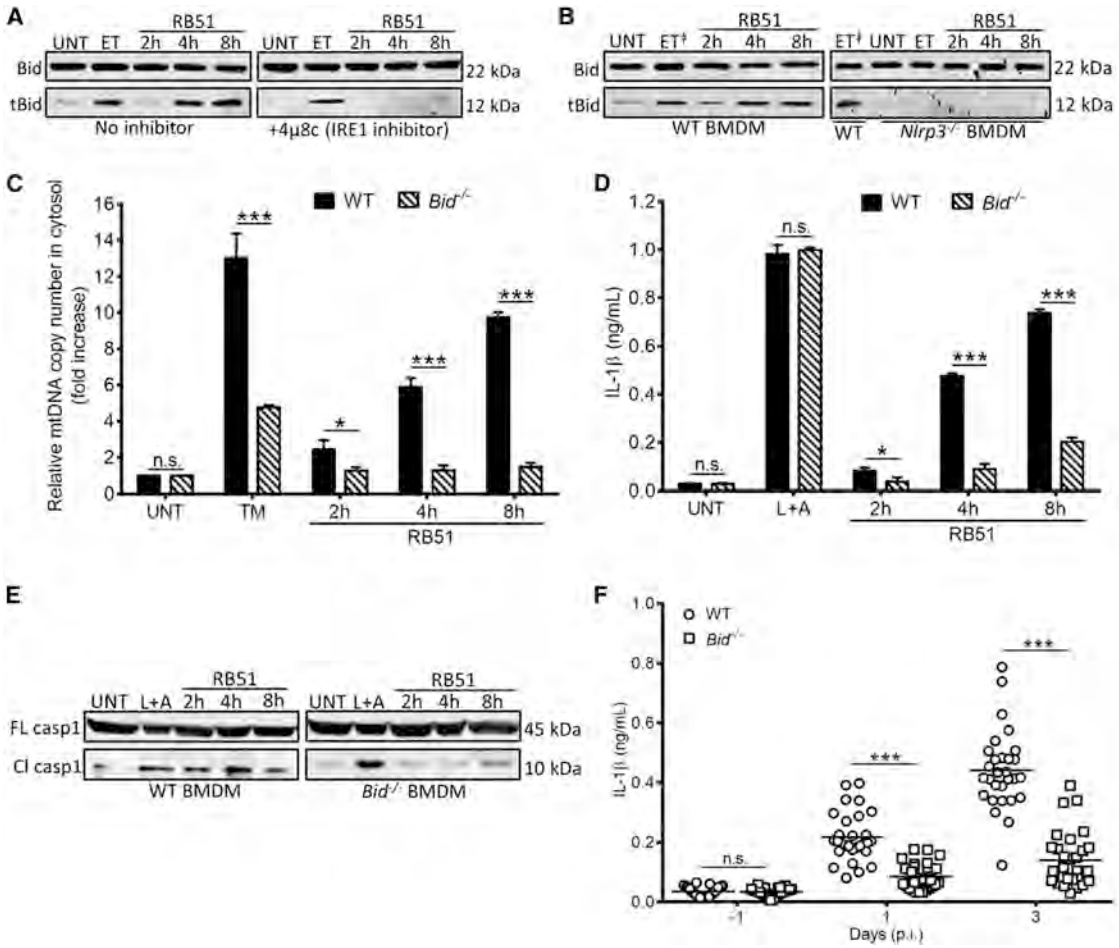

Figure 5. NLRP3 Controls Mitochondrial Dysfunction by a Bid-Dependent Mechanism

Bid truncation in RB51-infected (A) with or without 4μ8c (IRE1 inhibitor, 50 μM) and (B) WT and *Nlrp3*$^{-/-}$ BMDM – ET‡ identifies duplicate lanes of the same sample.

(C) Quantitative PCR of mtDNA in cytosolic extracts from RB51-infected WT and *Bid*$^{-/-}$ BMDM.

(D) ELISA of IL-1β in supernatants from RB51-infected WT and *Bid*$^{-/-}$ BMDM.

(E) Immunoblot analysis of caspase-1 in WT and *Bid*$^{-/-}$ BMDM infected with RB51.

(F) Serum IL-1β in WT (n = 29) and *Bid*$^{-/-}$ (n = 30) RB51-infected (i.p. CFU 1 × 10^8) mice. The data in (F) were pooled from two independent experiments. Error bars represent mean ± SD of n ≥ 3 independent experiments. * and *** represent p values of < 0.05 and < 0.0001, respectively. n.s., not significant. UNT, ET, TM, and L+A represent untreated, etoposide (positive control for Bid truncation, 25 μM), tunicamycin (positive control for ER stress induction, 10 μg/mL), and LPS+ATP (positive control for inflammasome activation, 200 ng/mL, and 1 mM) respectively. Immunoblots in (A), (B), and (E) are representative of n ≥ 3 independent experiments that were performed and imaged in parallel with identical parameters using a Li-Cor Odyssey imaging system. Full length (FL) caspase-1 and Bid serve as loading controls. See also Figure S5.

for BFA-induced inflammasome activation as previously reported by Tschopp and colleagues (Menu et al., 2012), perhaps due to more extensive perturbations in vesicular trafficking induced by BFA, compared to TM or TG, which act predominantly on the ER. In TM and TG-treated BMDM deficient in NLRP3, caspase-2, or Bid, caspase-1 cleavage was virtually absent (Figures 6C–6E). Although caspase-2 and Bid were critical for chemical ER stress-induced inflammasome activation, neither was required for inflammasome activation by LPS+ATP (Figures 6D and 6E). In total, our data support the IRE1-NLRP3-caspase2-Bid axis as a key mechanism by which ER stress drives mitochondrial damage and inflammasome activation.

DISCUSSION

ER stress is increasingly implicated in human disease, including infection, Alzheimer's disease, and diabetes (Wang and Kaufman, 2012). More recent studies have demonstrated a connection between ER stress and the inflammasome, although the mechanisms that control signaling have not been fully elucidated (Lerner et al., 2012; Menu et al., 2012; Oslowski et al., 2012). Our results have revealed that activation of the IRE1 ER stress sensor leads to NLRP3-mediated crosstalk between ER and mitochondria, resulting in release of mitochondrial contents through activation of the caspase-2-Bid signaling axis. Notably, the requirement of NLRP3 in ER stress-induced mitochondrial damage was

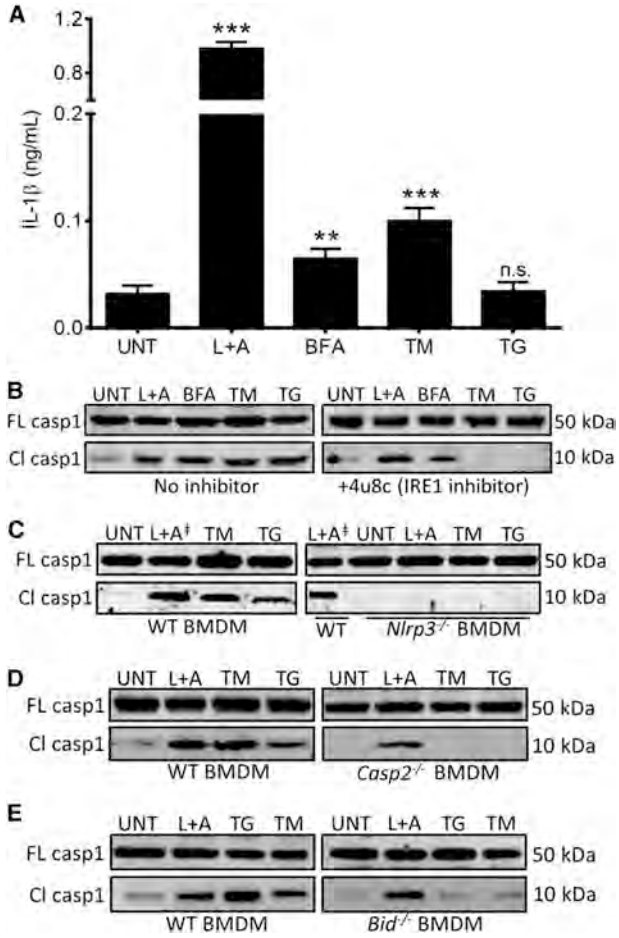

Figure 6. NLRP3 and Caspase-2 Are Required for Caspase-1 Activation during General ER Stress

(A) ELISA analysis of IL-1β in supernatants from BMDM treated with 200 ng/mL LPS and 1mM ATP, positive control for inflammasome activation), or the ER stressors BFA (brefeldin A, 20 μM), TM (tunicamycin, 10 μg/mL), and TG (thapsigargin, 10 μM). Error bars represent mean ± SD of n ≥ 3 independent experiments. ** and *** represent p values of < 0.001 and < 0.0001 respectively. n.s., not significant.

(B–E) Immunoblot analysis of caspase-1 in (B) BMDM in the absence or presence of 4μ8c (IRE1 inhibitor, 50 μM), (C) WT and *Nlrp3*$^{-/-}$ BMDM – L+A‡ identifies duplicate lanes of the same sample, (D) WT and *Casp2*$^{-/-}$ BMDM, and (E) WT and *Bid*$^{-/-}$ BMDM. Immunoblots in (B)–(E) are representative of n ≥ 3 independent experiments that were performed and imaged in parallel with identical parameters using a Li-Cor Odyssey imaging system. Full-length (FL) caspase-1 serves as a loading control. See also Figure S6.

independent of ASC and caspase-1, suggesting that this is not a function of the canonical NLRP3 inflammasome. Our data place NLRP3 upstream of caspase-2 in the ER-mitochondrial signaling pathway and provide a mechanism by which NLRP3 can facilitate mitochondrial damage to activate the inflammasome. Whether NLRP3 or additional inflammasome regulators act as downstream sensors of mitochondrial damage in ER stress conditions remains to be determined.

The role of mitochondria in activating inflammasomes has been somewhat controversial. Previously, K^+ efflux was proposed as the common mechanism by which diverse stresses that increase membrane permeability, e.g., bacterial toxins or LPS+ATP, activate the NLRP3 inflammasome without requiring mitochondrial damage (Allam et al., 2014; Muñoz-Planillo et al., 2013). Other studies have reported that mitochondrial damage is critical for inflammasome activation by LPS+ATP or by cytosolic DNA (Nakahira et al., 2011; Shimada et al., 2012). Further increasing the complexity of cellular stress signaling, ROS generated by NADPH oxidase and mitochondrial ROS might stimulate the inflammasome by different pathways (Martinon, 2010; Wynosky-Dolfi et al., 2014). In the conditions we used, NLRP3-dependent inflammasome activation by LPS+ATP was essentially independent of IRE1, caspase-2, Bid, or mitochondrial content release. However, ER stress-induced inflammasome activation required mitochondrial damage. To reconcile our results with previously published reports, we speculate that NLRP3-dependent oligomerization, necessary for inflammasome activation, might exhibit distinct signaling requirements depending on the type or magnitude of stress. A stress that initiates strong K^+ efflux, such as pore formation by bacterial toxins or pannexin-1 might allow cytosolic NLRP3 oligomerization, without mitochondrial damage and would therefore not be blocked by cyclosporin A (Kanneganti et al., 2007; Pelegrin and Surprenant, 2006). Stress that triggers weaker K^+ efflux might be more dependent on mitochondrial danger signals in order for NLRP3 to use the mitochondria as a platform for oligomerization. Thus, both quality and quantity of a given stress inducer (i.e., infection, chemical stressors, LPS+ATP) might define the critical circuits that are integrated to generate inflammatory output. NLRP3 has previously been shown to bind the mitochondrial phospholipid, cardiolipin, which is exposed on the cytosolic face of mitochondria upon oxidation (Iyer et al., 2013; Korytowski et al., 2011). Cardiolipin-enriched domains have been proposed to act as signaling platforms on the mitochondria, somewhat analogous to the manner in which cholesterol-enriched microdomains act as signaling platforms in the plasma membrane (Schug and Gottlieb, 2009). Notably, protocol-specific conditions might be critical in defining the reliance of inflammasome activation on K^+ efflux versus mitochondrial damage (Horng, 2014; Nakahira et al., 2011; Shimada et al., 2012). In fact, we found that differing times and concentrations of LPS+ATP treatments resulted in substantially different amounts of mtDNA release, perhaps providing an explanation for why conflicting results have been reported for the reliance of LPS+ATP on mitochondrial damage. The molecular context of cellular stress will likely be critical in defining key principles that govern NLRP3 inflammasome activation.

Microbial infection imposes complex stress conditions upon infected cells that are not fully defined for most microbes, but might include K^+ efflux, nutrient deprivation, cytoskeletal perturbations, and ROS generation. Microbes or microbial ligands activate IRE1 through TLR signaling (Martinon et al., 2010), and in vivo data clearly show that XBP1, a component of the IRE1 signaling pathway, and NLRP3 can mediate resistance to microbial infection (Martinon et al., 2010; von Moltke et al., 2013). These observations are consistent with the idea that activation of ER stress machinery influences the outcome of infection by tuning inflammatory responses. Importantly, a recent study demonstrated that IRE1 is required for optimal secretion of pro-inflammatory cytokines, including IL-1β, in a mouse model

of inflammatory arthritis (Qiu et al., 2013). Cellular stress in the form of ER perturbation and mitochondrial dysfunction may provide critical contextual danger signals that together with microbial ligands provoke robust immunity. Because ER stress and mitochondrial dysfunction are also associated with type 2 diabetes, obesity, Crohn's disease, and cancer (Escames et al., 2012; Garg et al., 2012), it will be of interest to determine whether the NLRP3-caspase-2 regulatory axis is more broadly involved in sterile inflammatory diseases.

NLRP3 has emerged as a critical regulator of the inflammasome in response to ER stress and IRE1 activation. How IRE1 leads to NLRP3-dependent stimulation of caspase-2 is still unclear. NLRP3 binds to the signaling adaptor, TXNIP, whose translation is controlled by activated IRE1 (Lerner et al., 2012; Oslowski et al., 2012; Zhou et al., 2010), suggesting that interaction as a possible interface that might lead to recruitment and cleavage of caspase-2. Alternatively, NLRP3 might interact with an accessory protein similar to ASC that recruits caspase-2 through its CARD domain. IRE1 itself is reported to modulate caspase-2 total protein amounts by controlling degradation of regulatory microRNAs in BFA, TG, or TM-treated murine embryonic fibroblasts (Upton et al., 2012). However, a recent report indicated that overall caspase-2 amounts do not change in response to ER stress induced in human leukemia- and lymphoma-derived cell lines (Sandow et al., 2014), which is consistent with our data in macrophages showing that caspase-2 cleavage, rather than increased caspase-2 protein, is the key parameter induced by ER stressors. Our results emphasize the requirement for NLRP3, caspase-2, and mitochondrial damage in triggering caspase-1 activation specifically in conditions of ER stress and lay the groundwork for investigating ER stress modulation as a therapeutic strategy for diseases of inflammation and immunity.

EXPERIMENTAL PROCEDURES

Mice

Humane animal care at the University of Michigan is provided by the Unit for Lab Animal Medicine, which is accredited by the American Association for Accreditation of Laboratory Animal Care and the Department of Health and Human Services. This study was carried out in strict accordance with the recommendations in the Guide for the Care and Use of Laboratory Animals of the National Institutes of Health. The protocol was approved by the Committee on the Care and Use of Animals (UCUCA) of the University of Michigan.

Bid WT (n = 29), *Bid*$^{-/-}$ (Yin et al., 1999) (n = 30), DMSO treated (n = 15), 4μ8c treated (n = 15), casp2 WT (n = 15), and *Casp2*$^{-/-}$ (n = 15) mice (8 −12 weeks) were injected intraperitoneally (i.p.) with *Brucella abortus* RB51 vaccine strain (1×10^8 CFU) in 200 μl of phosphate-buffered saline (PBS). Mice were matched by sex and age. Mice were treated with DMSO (5% in PBS) or 4μ8c (25 mg/kg) daily in 200 μl of PBS. Blood was collected by saphenous vein on day −1, 1, and 3 days pi. Serum was extracted from blood by centrifugation for 3 min at 10,000 rpm and used for assessing IL-1β production by ELISA. At day 3 pi, spleens were removed from euthanized mice, homogenized in 1 ml 0.2% NP-40, and serial dilutions plated onto *Brucella* agar plates to enumerate CFU.

Cell Culture and Infection

BMDM were isolated from WT, *Casp2*$^{-/-}$, *Asc*$^{-/-}$, *Nlrp3*$^{-/-}$, *Bid*$^{-/-}$, and *Aim2*$^{-/-}$ mice. *Casp2*$^{-/-}$ with corresponding WT were purchased from Jackson Laboratories (stock #007899) (Bergeron et al., 1998). *Nlrp3*$^{-/-}$ (Kanneganti et al., 2006) and *Asc*$^{-/-}$ (Ozören et al., 2006) were maintained by the Nuñez laboratory. *Bid*$^{-/-}$ (Yin et al., 1999) and corresponding WT mice were maintained by the Yin laboratory. *Aim2*$^{-/-}$ (Rathinam et al., 2010) and corresponding WT mice were maintained by the Fitzgerald laboratory (University of Massachusetts, Worcester).

Isolated BMDM were differentiated in DMEM (GIBCO) supplemented with 20% heat-inactivated FBS (Invitrogen), 1% L-glutamine (2 mM), 1% sodium pyruvate (1 mM), 0.1% β-mercaptoethanol (55 μM), and 30% L-929 conditioned medium. BMDM were cultured in non-TC treated plates at 37°C in 5% CO_2, fed fresh media on day 3, and harvested on day 6. Four million RAW264.7 macrophages or BMDM were seeded in 6 well plates 18 hr prior to infection. The LPS+ATP samples were pretreated with LPS (200 ng/mL) overnight, followed by treatment with 1 mM ATP as described below. The following day, where indicated, cells were pretreated with 10 μM cyclosporin A, 300 μM TUDCA, 50 μM 4μ8c, or 2 μM Y-VAD-CHO for 1 hr prior to infection. Untreated and pretreated cells were infected with RB51 (MOI 200) for 30 min, after which inoculum was removed and cells were washed with PBS. Medium containing 50 μg/ml gentamicin was added to kill extracellular bacteria. To synchronize infection, we spun cells at 1200 rpm for 3 min after adding inoculum. Cells were treated with 25 μM etoposide, 10 μM thapsigargin, 10 μg/mL tunicamycin, 20 μM brefeldin A, or 1 mM ATP for 4 hr. At the indicated times, cells were lysed in buffer containing 1% NP-40 on ice for 15 min and spun at 16,000 x *g* for 15 min to pellet the insoluble fraction. Soluble fractions were used for immunoblot assays. The insoluble fraction was resuspended in mitochondrial suspension buffer (10 mM TrisHCl pH 6.7, 0.15 mM $MgCl_2$, 0.25 sucrose, 1 mM PMSF, 1 mM DTT) and centrifuged at 11,000× *g* for 15 min at 4°C to pellet the isolated mitochondria. Purity of isolated mitochondria was assessed by immunoblotting for compartment-specific markers: calreticulin (ER), TOM20 (mitochondria), Lamin B1 (nucleus), and Actin (cytosol).

Bacterial Strains and Reagents

Brucella abortus strain RB51 was obtained from Dr. G. Schurig (Virginia Polytechnic Institute and State University). Reagents were obtained from the following vendors: Sigma-Aldrich (cyclosporin A, tunicamycin, etoposide, brefeldin A, ATP), Fisher (thapsigargin), Calbiochem (TUDCA), Axon (4μ8c), and SCBT (Y-VAD-CHO). Antibodies were obtained from the following vendors: SCBT (anti-p-PERK sc-32577; anti-ATF6 sc-22799; anti-caspase-1 sc-514; anti-TOM20 sc-11415; anti-Lamin-b1 sc-20682), Cell Signaling (anti-PERK 3192S; anti-IRE1 3294S; anti-cytochrome c 4272S; anti-Bid 2003S; anti-Calreticulin 2891), Fisher (anti-NLRP3 MAB7578), BioVision (anti-caspase-2 3027-100), and Thermo Scientific (anti-Actin MS1295P1).

Lentivirus Production and Silencing of *Ern1*

HEK293T cells were grown in DMEM with 10% fetal bovine serum (Invitrogen). Lentivirus particles were produced by transfecting the cells with the TRC shRNA encoding plasmid (pLKO.1) along with the packaging plasmids (pVSV-G, pGAG-PAL) obtained from the University of Michigan Vector Core. The medium was changed after 24 hr, and virus particles collected at 48 hr. Virus-containing medium was concentrated 10-fold by centrifugation (24,000 rpm) for 2 hr at 4°C. Concentrated virus was used to transduce RAW264.7 cells seeded in 60 mm dishes. The medium was changed 24 hr post transduction, and cells were left to grow for an additional 24 hr. Transduced cells were selected with puromycin (4 μg/mL) using vectors containing sequence from a mouse *Ern1*-specific shRNA plasmid (Open Biosystems: antisense sequence 5′-TTTCTCTATCAATTCACGAGC-3′) or a non-targeted control shRNA plasmid (Sigma-Aldrich).

Transient Silencing of *Txnip* and *Xbp1*

Immortalized BMDM were transfected with specific Dharmacon siGENOME *Txnip* siRNA (cat# M-040441-01-0005), *Xbp1* (cat.# M-040825-00-0005), or non-targeted siRNA (cat.# D-001206-13-20) using DharmaFECT4 transfection reagent according to the manufacturer's protocol. Silencing efficiency was assessed via immunoblot using anti-TXNIP (cat.# NBP1-54578, Novus Biologicals) and anti-XBP1 (cat.# ab37152, Abcam) antibodies.

ROS Measurements

BMDM were plated in a 96 well plate with black slides and clear bottom. At designated time points, BMDM were washed with PBS and then incubated with CM-H_2DCFDA (Invitrogen) at a final concentration of 2.5 μM in Ringer buffer (155 mM NaCl, 5 mM KCl, 1 mM $MgCl_2$ $6H_2O$, 2 mM NaH_2PO_4 H_2O,

10 mM HEPES, 10 mM glucose). Cell were incubated for 30 min at 37°C, washed 3 times with cold PBS, and incubated for an additional 15 min at 37°C in warm medium for recovery. After recovery, cells were washed one more time with PBS. Florescence was measured at excitation/emission 485nm/525nm.

Immunoblot Assay

Cytosolic extracts were separated by SDS-PAGE, transferred to nitrocellulose membranes (Millipore), blocked with 5% nonfat dry milk in TBS-0.1% Tween20 (TBS-T), and incubated overnight at 4°C with primary antibodies specified above. Membranes were washed with TBS-T and incubated with secondary IRDye 680LT Goat anti-rabbit or IRDye 680LT Goat anti-mouse (1:20,000) at room temperature for 1 hr. Bands were visualized using the Li-Cor Odyssey Infrared Imaging System. Immunoblots shown in the figures are representative of $n \geq 3$ independent experiments. All immunoblots shown within an individual panel were analyzed in parallel with identical parameters using the Li-Cor System.

Cytokine Analysis

Culture supernatants were collected at indicated time points from macrophages infected as described. IL-1β concentrations were determined by sandwich ELISA per manufacturer's instructions (BioLegend). A minimum of three technical replicates per experiment and three experimental replicates were analyzed for each condition.

Xbp1 Splicing Assay

Total RNA (2 μg) extracted from samples was prepared using the RNeasy Mini Kit (QIAGEN) and used for cDNA synthesis. Primers encompassing the spliced sequences in *Xbp1* mRNA (F: 5′-GAACCAGGAGTTAAGAACACG-3′ and R: 5′-AGGCAACAGTGTCAGAGTCC-3′) were used for PCR amplification with GoTaq polymerase (Invitrogen), with amplification using 30 cycles at 94°C 1 min, 60°C 1 min, and 72°C 1 min. PCR products were incubated with PstI (Invitrogen) at 37°C overnight, and separated by electrophoresis (2.5% agarose gel).

Mitochondrial DNA Release Assay

DNA was isolated from 200 μl of the cytosolic fraction using a DNeasy Blood & Tissue Kit (QIAGEN). Quantitative PCR was employed to measure mtDNA using Brilliant II SYBR Green with Low ROX (Agilent Technologies) on a Stratagene MX300 QPCR System. The copy number of mtDNA encoding cytochrome c oxidase I was normalized to nuclear DNA encoding 18S ribosomal RNA. The following primers were used: cytochrome c oxidase I (F: 5′-GCCCCAGATATAGCATTCCC-3′ and R: 5′-GTTCATCCTGTTCCTGCTCC-3′) and 18S rRNA (F: 5′-TAGAGGGACAAGTGGCGTTC-3′ and R: 5′-CGCTG AGCCAGTCAGTGT-3′).

Lactate Dehydrogenase Release Assay

Macrophages were seeded in 96-well plates and infected with RB51 as above. Supernatants were analyzed for LDH enzyme using the CytoTox-ONE Homogeneous Membrane Integrity Assay (Promega) per manufacturer's instructions. Percentage LDH release was calculated as 100 X [(Experimental LDH Release – Culture Medium Background)/(Maximum LDH Release – Culture Medium Background)].

Statistical Analysis

All p values were generated between identified samples using unpaired two-tailed Student's t tests and represent analysis of ≥ 3 replicates per condition. Asterisks denote the following p values: *$p < 0.05$, **$p < 0.001$, and ***$p < 0.0001$.

SUPPLEMENTAL INFORMATION

Supplemental Information includes six figures and can be found with this article online at http://dx.doi.org/10.1016/j.immuni.2015.08.008.

AUTHOR CONTRIBUTIONS

D.N.B., Y.H., and M.X.D.O. designed the experiments. D.N.B., B.H.A., and M.X.D.O. performed the experiments. B.H.A., K.A.F., G.N., Y.H., X.C., and X.-M.Y. contributed critical reagents, materials, and discussion. D.N.B. and M.X.D.O. analyzed the data and wrote the paper.

ACKNOWLEDGMENTS

We acknowledge members of the M.X.D.O. laboratory for helpful discussions. We thank Drs. D. Monack and V. Carruthers for critical review of the manuscript. We are grateful to Dr. M. Swanson, Dr. V. Rathinam, Dr. Yuan He, and Dr. D. Ron for providing critical reagents and experimental guidance. We thank the staff of the UM Unit for Laboratory Animal Medicine. The University of Michigan Vector Core provided the TRC shRNA plasmids for *Ern1* silencing. We acknowledge financial support from the University of Michigan Rackham Graduate School (Y.H. and D.N.B.), the UM Genetics Training Program (D.N.B., GM007544), the UM Lung Immunopathology Training Program (B.H.A., HL007517), and the American Heart Association (B.H.A.). This research was supported by funding from the NIH to M.X.D.O. (AI101777), K.A.F. (AI083713), G.N. (AI063331, AR059688), X.-M.Y. (AA021751), and the University of Michigan Medical School Unit for Laboratory Animal Medicine and Endowment for Basic Science (Y.H.). The funders had no role in study design, data collection, and analysis, decision to publish, or preparation of the manuscript.

Received: July 28, 2014
Revised: June 1, 2015
Accepted: July 28, 2015
Published: September 1, 2015

REFERENCES

Allam, R., Lawlor, K.E., Yu, E.C., Mildenhall, A.L., Moujalled, D.M., Lewis, R.S., Ke, F., Mason, K.D., White, M.J., Stacey, K.J., et al. (2014). Mitochondrial apoptosis is dispensable for NLRP3 inflammasome activation but non-apoptotic caspase-8 is required for inflammasome priming. EMBO Rep. *15*, 982–990.

Bergeron, L., Perez, G.I., Macdonald, G., Shi, L., Sun, Y., Jurisicova, A., Varmuza, S., Latham, K.E., Flaws, J.A., Salter, J.C., et al. (1998). Defects in regulation of apoptosis in caspase-2-deficient mice. Genes Dev. *12*, 1304–1314.

Bischof, L.J., Kao, C.Y., Los, F.C., Gonzalez, M.R., Shen, Z., Briggs, S.P., van der Goot, F.G., and Aroian, R.V. (2008). Activation of the unfolded protein response is required for defenses against bacterial pore-forming toxin in vivo. PLoS Pathog. *4*, e1000176.

Bronner, D.N., O'Riordan, M.X., and He, Y. (2013). Caspase-2 mediates a Brucella abortus RB51-induced hybrid cell death having features of apoptosis and pyroptosis. Front. Cell. Infect. Microbiol. *3*, 83.

Brown, M.K., and Naidoo, N. (2012). The endoplasmic reticulum stress response in aging and age-related diseases. Front. Physiol. *3*, 263.

Chen, F., and He, Y. (2009). Caspase-2 mediated apoptotic and necrotic murine macrophage cell death induced by rough Brucella abortus. PLoS ONE *4*, e6830.

Cross, B.C., Bond, P.J., Sadowski, P.G., Jha, B.K., Zak, J., Goodman, J.M., Silverman, R.H., Neubert, T.A., Baxendale, I.R., Ron, D., and Harding, H.P. (2012). The molecular basis for selective inhibition of unconventional mRNA splicing by an IRE1-binding small molecule. Proc. Natl. Acad. Sci. USA *109*, E869–E878.

Davis, B.K., Wen, H., and Ting, J.P. (2011). The inflammasome NLRs in immunity, inflammation, and associated diseases. Annu. Rev. Immunol. *29*, 707–735.

Escames, G., López, L.C., García, J.A., García-Corzo, L., Ortiz, F., and Acuña-Castroviejo, D. (2012). Mitochondrial DNA and inflammatory diseases. Hum. Genet. *131*, 161–173.

Garg, A.D., Kaczmarek, A., Krysko, O., Vandenabeele, P., Krysko, D.V., and Agostinis, P. (2012). ER stress-induced inflammation: does it aid or impede disease progression? Trends Mol. Med. *18*, 589–598.

Gomes, M.T., Campos, P.C., Oliveira, F.S., Corsetti, P.P., Bortoluci, K.R., Cunha, L.D., Zamboni, D.S., and Oliveira, S.C. (2013). Critical role of ASC

inflammasomes and bacterial type IV secretion system in caspase-1 activation and host innate resistance to Brucella abortus infection. J. Immunol. *190*, 3629–3638.

Handschumacher, R.E., Harding, M.W., Rice, J., Drugge, R.J., and Speicher, D.W. (1984). Cyclophilin: a specific cytosolic binding protein for cyclosporin A. Science *226*, 544–547.

Hao, L.Y., Liu, X., and Franchi, L. (2013). Inflammasomes in inflammatory bowel disease pathogenesis. Curr. Opin. Gastroenterol. *29*, 363–369.

Hetz, C. (2012). The unfolded protein response: controlling cell fate decisions under ER stress and beyond. Nat. Rev. Mol. Cell Biol. *13*, 89–102.

Hitomi, J., Katayama, T., Eguchi, Y., Kudo, T., Taniguchi, M., Koyama, Y., Manabe, T., Yamagishi, S., Bando, Y., Imaizumi, K., et al. (2004). Involvement of caspase-4 in endoplasmic reticulum stress-induced apoptosis and Abeta-induced cell death. J. Cell Biol. *165*, 347–356.

Horng, T. (2014). Calcium signaling and mitochondrial destabilization in the triggering of the NLRP3 inflammasome. Trends Immunol. *35*, 253–261.

Iyer, S.S., He, Q., Janczy, J.R., Elliott, E.I., Zhong, Z., Olivier, A.K., Sadler, J.J., Knepper-Adrian, V., Han, R., Qiao, L., et al. (2013). Mitochondrial cardiolipin is required for Nlrp3 inflammasome activation. Immunity *39*, 311–323.

Jesenberger, V., Procyk, K.J., Yuan, J., Reipert, S., and Baccarini, M. (2000). Salmonella-induced caspase-2 activation in macrophages: a novel mechanism in pathogen-mediated apoptosis. J. Exp. Med. *192*, 1035–1046.

Kanneganti, T.D., Ozören, N., Body-Malapel, M., Amer, A., Park, J.H., Franchi, L., Whitfield, J., Barchet, W., Colonna, M., Vandenabeele, P., et al. (2006). Bacterial RNA and small antiviral compounds activate caspase-1 through cryopyrin/Nalp3. Nature *440*, 233–236.

Kanneganti, T.D., Lamkanfi, M., Kim, Y.G., Chen, G., Park, J.H., Franchi, L., Vandenabeele, P., and Núñez, G. (2007). Pannexin-1-mediated recognition of bacterial molecules activates the cryopyrin inflammasome independent of Toll-like receptor signaling. Immunity *26*, 433–443.

Kono, H., and Rock, K.L. (2008). How dying cells alert the immune system to danger. Nat. Rev. Immunol. *8*, 279–289.

Korsmeyer, S.J., Wei, M.C., Saito, M., Weiler, S., Oh, K.J., and Schlesinger, P.H. (2000). Pro-apoptotic cascade activates BID, which oligomerizes BAK or BAX into pores that result in the release of cytochrome c. Cell Death Differ. *7*, 1166–1173.

Korytowski, W., Basova, L.V., Pilat, A., Kernstock, R.M., and Girotti, A.W. (2011). Permeabilization of the mitochondrial outer membrane by Bax/truncated Bid (tBid) proteins as sensitized by cardiolipin hydroperoxide translocation: mechanistic implications for the intrinsic pathway of oxidative apoptosis. J. Biol. Chem. *286*, 26334–26343.

Lee, H.Y., Choi, C.S., Birkenfeld, A.L., Alves, T.C., Jornayvaz, F.R., Jurczak, M.J., Zhang, D., Woo, D.K., Shadel, G.S., Ladiges, W., et al. (2010). Targeted expression of catalase to mitochondria prevents age-associated reductions in mitochondrial function and insulin resistance. Cell Metab. *12*, 668–674.

Lerner, A.G., Upton, J.P., Praveen, P.V., Ghosh, R., Nakagawa, Y., Igbaria, A., Shen, S., Nguyen, V., Backes, B.J., Heiman, M., et al. (2012). IRE1α induces thioredoxin-interacting protein to activate the NLRP3 inflammasome and promote programmed cell death under irremediable ER stress. Cell Metab. *16*, 250–264.

Li, X., and He, Y. (2012). Caspase-2-dependent dendritic cell death, maturation, and priming of T cells in response to Brucella abortus infection. PLoS ONE *7*, e43512.

Martinon, F. (2010). Signaling by ROS drives inflammasome activation. Eur. J. Immunol. *40*, 616–619.

Martinon, F., Chen, X., Lee, A.H., and Glimcher, L.H. (2010). TLR activation of the transcription factor XBP1 regulates innate immune responses in macrophages. Nat. Immunol. *11*, 411–418.

Menu, P., Mayor, A., Zhou, R., Tardivel, A., Ichijo, H., Mori, K., and Tschopp, J. (2012). ER stress activates the NLRP3 inflammasome via an UPR-independent pathway. Cell Death Dis. *3*, e261.

Muñoz-Planillo, R., Kuffa, P., Martínez-Colón, G., Smith, B.L., Rajendiran, T.M., and Núñez, G. (2013). K^+ efflux is the common trigger of NLRP3 inflammasome activation by bacterial toxins and particulate matter. Immunity *38*, 1142–1153.

Nakahira, K., Haspel, J.A., Rathinam, V.A., Lee, S.J., Dolinay, T., Lam, H.C., Englert, J.A., Rabinovitch, M., Cernadas, M., Kim, H.P., et al. (2011). Autophagy proteins regulate innate immune responses by inhibiting the release of mitochondrial DNA mediated by the NALP3 inflammasome. Nat. Immunol. *12*, 222–230.

Olden, K., Pratt, R.M., and Yamada, K.M. (1978). Role of carbohydrates in protein secretion and turnover: effects of tunicamycin on the major cell surface glycoprotein of chick embryo fibroblasts. Cell *13*, 461–473.

Oslowski, C.M., Hara, T., O'Sullivan-Murphy, B., Kanekura, K., Lu, S., Hara, M., Ishigaki, S., Zhu, L.J., Hayashi, E., Hui, S.T., et al. (2012). Thioredoxin-interacting protein mediates ER stress-induced β cell death through initiation of the inflammasome. Cell Metab. *16*, 265–273.

Ozören, N., Masumoto, J., Franchi, L., Kanneganti, T.D., Body-Malapel, M., Ertürk, I., Jagirdar, R., Zhu, L., Inohara, N., Bertin, J., et al. (2006). Distinct roles of TLR2 and the adaptor ASC in IL-1beta/IL-18 secretion in response to Listeria monocytogenes. J. Immunol. *176*, 4337–4342.

Pelegrin, P., and Surprenant, A. (2006). Pannexin-1 mediates large pore formation and interleukin-1beta release by the ATP-gated P2X7 receptor. EMBO J. *25*, 5071–5082.

Pillich, H., Loose, M., Zimmer, K.P., and Chakraborty, T. (2012). Activation of the unfolded protein response by Listeria monocytogenes. Cell. Microbiol. *14*, 949–964.

Qiu, Q., Zheng, Z., Chang, L., Zhao, Y.S., Tan, C., Dandekar, A., Zhang, Z., Lin, Z., Gui, M., Li, X., et al. (2013). Toll-like receptor-mediated IRE1α activation as a therapeutic target for inflammatory arthritis. EMBO J. *32*, 2477–2490.

Rathinam, V.A., Jiang, Z., Waggoner, S.N., Sharma, S., Cole, L.E., Waggoner, L., Vanaja, S.K., Monks, B.G., Ganesan, S., Latz, E., et al. (2010). The AIM2 inflammasome is essential for host defense against cytosolic bacteria and DNA viruses. Nat. Immunol. *11*, 395–402.

Robertson, J.D., Enoksson, M., Suomela, M., Zhivotovsky, B., and Orrenius, S. (2002). Caspase-2 acts upstream of mitochondria to promote cytochrome c release during etoposide-induced apoptosis. J. Biol. Chem. *277*, 29803–29809.

Sandow, J.J., Dorstyn, L., O'Reilly, L.A., Tailler, M., Kumar, S., Strasser, A., and Ekert, P.G. (2014). ER stress does not cause upregulation and activation of caspase-2 to initiate apoptosis. Cell Death Differ. *21*, 475–480.

Saxena, G., Chen, J., and Shalev, A. (2010). Intracellular shuttling and mitochondrial function of thioredoxin-interacting protein. J. Biol. Chem. *285*, 3997–4005.

Schroder, K., and Tschopp, J. (2010). The inflammasomes. Cell *140*, 821–832.

Schug, Z.T., and Gottlieb, E. (2009). Cardiolipin acts as a mitochondrial signalling platform to launch apoptosis. Biochim. Biophys. Acta *1788*, 2022–2031.

Seimon, T.A., Kim, M.J., Blumenthal, A., Koo, J., Ehrt, S., Wainwright, H., Bekker, L.G., Kaplan, G., Nathan, C., Tabas, I., and Russell, D.G. (2010). Induction of ER stress in macrophages of tuberculosis granulomas. PLoS ONE *5*, e12772.

Shimada, K., Crother, T.R., Karlin, J., Dagvadorj, J., Chiba, N., Chen, S., Ramanujan, V.K., Wolf, A.J., Vergnes, L., Ojcius, D.M., et al. (2012). Oxidized mitochondrial DNA activates the NLRP3 inflammasome during apoptosis. Immunity *36*, 401–414.

Sidrauski, C., and Walter, P. (1997). The transmembrane kinase Ire1p is a site-specific endonuclease that initiates mRNA splicing in the unfolded protein response. Cell *90*, 1031–1039.

Subramanian, N., Natarajan, K., Clatworthy, M.R., Wang, Z., and Germain, R.N. (2013). The adaptor MAVS promotes NLRP3 mitochondrial localization and inflammasome activation. Cell *153*, 348–361.

Tan, M.S., Yu, J.T., Jiang, T., Zhu, X.C., and Tan, L. (2013). The NLRP3 Inflammasome in Alzheimer's Disease. Mol Neurobiol.

Upton, J.P., Austgen, K., Nishino, M., Coakley, K.M., Hagen, A., Han, D., Papa, F.R., and Oakes, S.A. (2008). Caspase-2 cleavage of BID is a critical apoptotic signal downstream of endoplasmic reticulum stress. Mol. Cell. Biol. *28*, 3943–3951.

Upton, J.P., Wang, L., Han, D., Wang, E.S., Huskey, N.E., Lim, L., Truitt, M., McManus, M.T., Ruggero, D., Goga, A., et al. (2012). IRE1α cleaves select microRNAs during ER stress to derepress translation of proapoptotic Caspase-2. Science *338*, 818–822.

von Moltke, J., Ayres, J.S., Kofoed, E.M., Chavarría-Smith, J., and Vance, R.E. (2013). Recognition of bacteria by inflammasomes. Annu. Rev. Immunol. *31*, 73–106.

Wang, S., and Kaufman, R.J. (2012). The impact of the unfolded protein response on human disease. J. Cell Biol. *197*, 857–867.

Wang, X.Z., Kuroda, M., Sok, J., Batchvarova, N., Kimmel, R., Chung, P., Zinszner, H., and Ron, D. (1998). Identification of novel stress-induced genes downstream of chop. EMBO J. *17*, 3619–3630.

Wynosky-Dolfi, M.A., Snyder, A.G., Philip, N.H., Doonan, P.J., Poffenberger, M.C., Avizonis, D., Zwack, E.E., Riblett, A.M., Hu, B., Strowig, T., et al. (2014). Oxidative metabolism enables Salmonella evasion of the NLRP3 inflammasome. J. Exp. Med. *211*, 653–668.

Yin, X.M., Wang, K., Gross, A., Zhao, Y., Zinkel, S., Klocke, B., Roth, K.A., and Korsmeyer, S.J. (1999). Bid-deficient mice are resistant to Fas-induced hepatocellular apoptosis. Nature *400*, 886–891.

Yoshida, H., Matsui, T., Yamamoto, A., Okada, T., and Mori, K. (2001). XBP1 mRNA is induced by ATF6 and spliced by IRE1 in response to ER stress to produce a highly active transcription factor. Cell *107*, 881–891.

Zeng, Y., and Elbein, A.D. (1995). UDP-N-acetylglucosamine:dolichyl-phosphate N-acetylglucosamine-1-phosphate transferase is amplified in tunicamycin-resistant soybean cells. European journal of biochemistry / FEBS *233*, 458–466.

Zhang, Q., Kang, R., Zeh, H.J., 3rd, Lotze, M.T., and Tang, D. (2013). DAMPs and autophagy: cellular adaptation to injury and unscheduled cell death. Autophagy *9*, 451–458.

Zhou, R., Tardivel, A., Thorens, B., Choi, I., and Tschopp, J. (2010). Thioredoxin-interacting protein links oxidative stress to inflammasome activation. Nat. Immunol. *11*, 136–140.

Zhou, R., Yazdi, A.S., Menu, P., and Tschopp, J. (2011). A role for mitochondria in NLRP3 inflammasome activation. Nature *469*, 221–225.